



UNIVERSITY OF LEEDS

This is a repository copy of *Evaluating the potential of full-waveform lidar for mapping pan-tropical tree species richness*.

White Rose Research Online URL for this paper:
<https://eprints.whiterose.ac.uk/162817/>

Version: Accepted Version

Article:

Marselis, SM, Abernethy, K, Alonso, A et al. (29 more authors) (2020) Evaluating the potential of full-waveform lidar for mapping pan-tropical tree species richness. *Global Ecology and Biogeography*, 29 (10). pp. 1799-1816. ISSN 1466-822X

<https://doi.org/10.1111/geb.13158>

© 2020 John Wiley & Sons Ltd. This is the peer reviewed version of the following article: Marselis, SM, Abernethy, K, Alonso, A, et al. Evaluating the potential of full-waveform lidar for mapping pan-tropical tree species richness. *Global Ecol Biogeogr.* 2020; 00: 1– 18. <https://doi.org/10.1111/geb.13158> , which has been published in final form at <https://doi.org/10.1111/geb.13158>. This article may be used for non-commercial purposes in accordance with Wiley Terms and Conditions for Use of Self-Archived Versions. Uploaded in accordance with the publisher's self-archiving policy.

Reuse

Items deposited in White Rose Research Online are protected by copyright, with all rights reserved unless indicated otherwise. They may be downloaded and/or printed for private study, or other acts as permitted by national copyright laws. The publisher or other rights holders may allow further reproduction and re-use of the full text version. This is indicated by the licence information on the White Rose Research Online record for the item.

Takedown

If you consider content in White Rose Research Online to be in breach of UK law, please notify us by emailing eprints@whiterose.ac.uk including the URL of the record and the reason for the withdrawal request.



eprints@whiterose.ac.uk
<https://eprints.whiterose.ac.uk/>

1 **Title**

2 Evaluating the Potential of Full-waveform Lidar for Mapping Pan-Tropical Tree Species Richness

3

4 **Short title**

5 Lidar and Pan-Tropical Tree Species Richness

6

7 **Abstract**

8 **Aim:**

9 Mapping tree species richness across the tropics is of great interest for effective conservation and
10 biodiversity management to help prevent species extinction. In this study, we evaluated the potential of
11 full-waveform lidar data for mapping tree species richness across the tropics by relating measurements
12 of vertical canopy structure, as a proxy for the occupation of vertical niche space, to tree species
13 richness.

14 **Location:**

15 Tropics

16 **Time period:**

17 Present

18 **Major taxa studied:**

19 Trees

20 **Methods:**

21 First, we evaluated the characteristics of the vertical canopy structure across 15 study sites using
22 (simulated) full-waveform lidar data and related these findings to in-situ tree species information. Then,
23 we developed structure-richness models at the local (within 25-50 ha plots), regional (biogeographic
24 regions), and pan-tropical scale at three spatial resolutions (1.0, 0.25 and 0.0625 ha) using Poisson
25 regression.

26 **Results:**

27 The results showed a weak structure-richness relationship at the local scale. At the regional scale (within
28 a biogeographical region) a stronger relationship was found between canopy structure and tree species
29 richness across different tropical forest types, for example across Central Africa and in South America (R^2
30 ranging from 0.44-0.56, RMSD ranging between 23-61%). A weaker relationship was found at the pan-
31 tropical scale, including data across four continents ($R^2 = 0.39$ and RMSE = 43%, 0.25 ha resolution).

32 **Main Conclusions:**

33 Our results may serve as a basis for future development of a set of structure-richness models to map
34 high resolution tree species richness using vertical canopy structure information from the Global
35 Ecosystem Dynamics Investigation (GEDI). The value of this effort would be enhanced by access to a
36 larger set of field reference data for all tropical regions. Future research could also support the use of
37 GEDI canopy structure data in frameworks using environmental and spectral information for modelling
38 tree species richness across the tropics.

39 **Keywords**

40 Biodiversity, canopy structure, GEDI, lidar, plant area index, tropical forests

41 **1. Introduction**

42 Tropical forests are known for their high tree species diversity. Current estimates suggest in the order of
43 15,000 tree species in Amazonia alone, in contrast to 124 tree species in temperate forests in Europe,
44 and more than 40,000 different tree species across the tropical region (Slik *et al.*, 2015; Ter Steege *et al.*,
45 2015). High levels of tree species richness are essential for maximizing the provision of essential
46 ecosystem services (Liang *et al.*, 2016). Unfortunately, 35% of pre-agricultural global forest cover has
47 been lost over the past 300 years, largely due to increasing human pressures on the environment. 82%
48 of the remaining forest is estimated to have experienced some degree of human impact (Watson *et al.*,
49 2018). Current extinction rates are estimated to be at least 1000 times higher than background
50 extinction rates (Pimm *et al.*, 2014), and it was recently estimated that in the Amazonian tropics alone
51 approximately 25% of the tree species are threatened with extinction (Ter Steege *et al.*, 2015). The
52 Convention of Biological Diversity (CBD) and Group on Earth Observations Biodiversity Observation
53 Network (GEO BON) have developed a list of important variables aiming to provide quantitative
54 information on biodiversity to reach the Aichi biodiversity targets 2020 (Pereira *et al.*, 2013; Skidmore *et*
55 *al.*, 2015). Among the identified needs is the mapping of taxonomic diversity at high spatial resolution
56 over large scales (Pereira *et al.*, 2010). Here we focus on tree species diversity. The collection of tree
57 species diversity data is traditionally done in the field, and such information has previously been used to
58 create predictive maps of tree species richness across the globe at low spatial resolution (Kier *et al.*,
59 2005; Mutke & Barthlott, 2005). More recently, passive remote sensing data, such as optical imagery
60 from different airborne and spaceborne platforms, has been used in combination with field reference
61 data to predict tree species diversity in different regions (Foody & Cutler, 2006; Carlson *et al.*, 2007;
62 Féret & Asner, 2014; Rocchini *et al.*, 2016; Schäfer *et al.*, 2016; Bongalov *et al.*, 2019). Even though such
63 methods have been progressively developing over the last decade, they are not yet operational for

64 mapping tree species richness across the tropics due to, among others, a lack of consistent remote
65 sensing and training data over such scales, insufficient model accuracy and/or low spatial resolution.

66 The scientific community has called for bolder science in conservation strategies to enable effective
67 management of the Earth's forests and allow for better conservation of our natural ecosystems (Watson
68 *et al.*, 2016). In this study we focus on the use of active remote sensing, specifically lidar, for mapping
69 taxonomic tree species richness in the tropics. While local tropical forest diversity is largely independent
70 of biomass (Sullivan *et al.*, 2017), it remains unclear if substantial amounts of variation in species
71 diversity are associated with other features of forest structure. Here, we explore for the first time
72 whether small-scale vertical canopy structure variation is significantly associated with the spatial
73 variation in tropical tree species richness. On a global scale it has previously been shown that canopy
74 height explains a limited portion of the variation in tree species diversity, as such data provides
75 information on the available niche space (Gatti *et al.*, 2017). It has since been hypothesized that
76 including information on the vertical canopy structure, must explain more of the variation in tree
77 species diversity than canopy height alone; as such data provide information on the occupation of the
78 vertical niche space. Marselis *et al.*, (2019) demonstrated that information on canopy height and vertical
79 canopy structure, expressed as the Plant Area Index (PAI) profile from full-waveform airborne lidar data,
80 could be used to map tree species diversity in Gabon, Africa. However, it is not clear whether this
81 relationship is of similar nature and strength across different regions, or even the entire tropics. If
82 existent, than the use of such a structure-diversity relationship(s) could become operational at a pan-
83 tropical scale with the rapidly increasing availability of spaceborne canopy structure information derived
84 from the Global Ecosystem Dynamics Investigation (GEDI), a full-waveform spaceborne lidar system
85 (Dubayah *et al. under review*). GEDI is expected to provide over 10 billion measurements of vertical
86 canopy structure across the temperate and tropical forests between 2019 and 2021.

87 Factors influencing tree species diversity on a global scale differ from those affecting spatial patterns at
88 regional or local scales. In general, tropical tree species diversity increases with increasing precipitation,
89 forest stature, soil fertility, time since catastrophic disturbance and rate of canopy turnover and
90 decreases with seasonality, latitude, and altitude (Givnish, 1999). At large-grain scales historical
91 biogeography processes are more important, whereas at the plot-scale environmental variables strongly
92 influence diversity (Keil & Chase, 2019).

93 Similar to species diversity, forest structure at the global scale is influenced by interacting historic,
94 environmental, and human related variables; precipitation in the wettest month being the most
95 important single predictor of plant height (Moles *et al.*, 2009). Forest structure measured in the field is
96 mainly comprised of four variables: canopy height, biomass, basal area and tree density (Palace *et al.*,
97 2015). However, active remote sensing techniques have revolutionized the study of canopy structure
98 (Newnham *et al.*, 2015). With lidar remote sensing, for example, it is now possible to obtain information
99 on canopy height, as well as the position and amount of plant material along the vertical axis of the
100 canopy (Tang *et al.*, 2012). Palace *et al.* (2015) stressed that high resolution lidar data possess vertical
101 structure information which is inherently linked to ecological processes.

102 We hypothesize that structure-diversity relationships will vary across different biogeographical and
103 phylogenetic regions (Corlett & Primack, 2011; Slik *et al.*, 2018) and that it may be more fruitful to
104 develop multiple relationships rather than one pan-tropical relationship for operationalizing tree species
105 diversity mapping with spaceborne active remote sensing data. Additionally, the strength of the
106 relationship between a variable and tree species diversity often changes with resolution (plot size) as
107 tree species diversity is not linearly related with area (species-area curve) (MacArthur & Wilson, 1967).
108 This complicates the development of predictive models at specific resolutions, and also limits the
109 extrapolation of estimates at one resolution to a larger area, which impedes the mapping of pan-tropical
110 tree species diversity at high spatial resolution.

111 In sum, we know that both species diversity and canopy structure vary greatly within and across
112 continents. Hence, our objective is to assess whether canopy structure information can explain tree
113 species richness at the local, regional and/or global scale with the ultimate goal to evaluate the efficacy
114 of spaceborne full-waveform lidar for mapping tree species richness across the tropics. First, we
115 compare characteristics of the vertical canopy structure, measured with full-waveform lidar data, of
116 tropical forests across the world. Second, we evaluate the differences in species richness and species-
117 area curves across the different study sites using field measurements. Third, we evaluate the potential
118 for developing local (within 25-50 ha field plots), regional (within biogeographical regions) and pan-
119 tropical structure-richness relationships, relating canopy structure metrics from lidar to tree species
120 richness measurements from the field at three spatial resolutions (0.0625, 0.25 and 1.0 ha). Lastly, we
121 discuss the potential of full-waveform lidar data from GEDI for mapping tree species richness across the
122 tropics using structure-richness relationships.

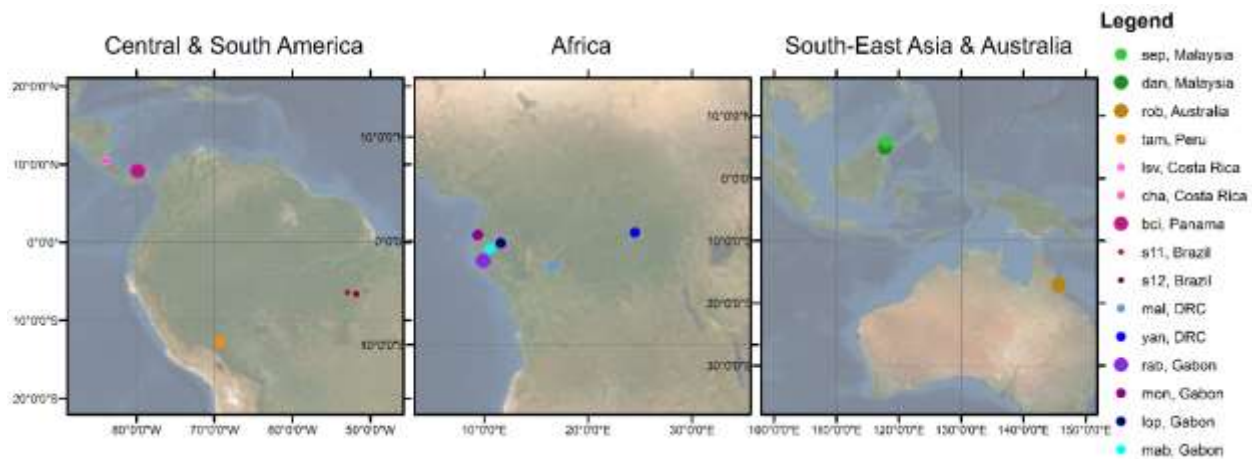
123 **2. Materials and Methods**

124 We address the relationship between canopy structure and tree species richness in *terra firme* forest in
125 the tropical region between 23.5° N & S. We compiled a comprehensive field and lidar dataset covering
126 colonizing forest, old-growth tropical forest and forests under different degrees of degradation and
127 savanna. We included such a wide variety of forest stages as most of the Earth's tropical forests have
128 been degraded or otherwise affected by natural and human influences (Lewis *et al.*, 2015). Hence, when
129 developing a method that allows for estimating pan-tropical tree species richness it is important to
130 include data from across this range of possibilities. Species diversity can be expressed with many
131 different metrics. Generally, three levels of diversity are recognized: α , β , and γ diversity. α diversity
132 refers to the local diversity of a community, habitat or field plot. β diversity refers to the differences in
133 diversity between habitats and γ diversity to the total diversity of a region (Colwell, 2009). In this study
134 we focus on α diversity. α diversity can be expressed with many different indicators. In this study we
135 focus on species richness (S) expressed as the total number of species in a plot of a given size. Hence,
136 from here on forward we only refer to tree species richness, used to express the local tree species
137 diversity.

138 **2.1 Field Datasets**

139 Field data were used to calculate the reference values of tree species richness. We used 15 datasets:
140 one from Australia, two from South-East Asia, six from Africa, three from South America and three from
141 Central America (Figure 1). All field datasets used in this study have been previously collected and
142 published and have coincident airborne lidar data available. Each field dataset is labeled with a three-
143 letter code and contained information on tree location, species and diameter at breast height (DBH). All
144 datasets were collected by different organizations and research teams resulting in different data
145 characteristics (Table 1, S11). Four datasets consisted of one large plot of 25 ha (*rob*, Australia and *rab*,

146 Gabon) or 50 ha (*dan*, Malaysia and *bci*, Panama). The other eleven datasets consisted of multiple (3-21)
147 smaller plots with sizes ranging from 0.16 ha to 4.0 ha.



148
149 *Figure 1: Location of field sites across the three continents, colors of each study site are consistent*
150 *throughout the paper. Gridlines indicate 10° intervals in longitudinal and latitudinal directions. The size*
151 *of the place markers represents the size of the total sampled area relative to each other.*

152

153 *Table 1: Information on the original plot size, the amount of total area sampled in the field and the*
 154 *source of the data which is either a website where the data are published and/or a publication in which*
 155 *the data are described further.*

Country	Project code	No. native plots	Total area (ha)	Source / Additional Information
Oceania				
Australia	<i>rob</i>	1	25	(Bradford <i>et al.</i> , 2014)
South-East Asia				
Malaysia	<i>dan</i>	1	50	https://forestgeo.si.edu/sites/asia/danum-valley
Malaysia	<i>sep</i>	9	36	https://www.forestplots.net/en/ (Jucker <i>et al.</i> , 2018)
Africa				
DRC	<i>mal</i>	21	21	(Bastin <i>et al.</i> , 2015)
DRC	<i>yan</i>	9	9	(Kearsley <i>et al.</i> , 2013)
Gabon	<i>rab</i>	1	25	https://forestgeo.si.edu/sites/africa/rabi (Memiaghe <i>et al.</i> , 2016)
Gabon	<i>lop</i>	11	9.5	https://www.forestplots.net/en/ (Labrière <i>et al.</i> , 2018)
Gabon	<i>mon</i>	10	10	(Fatoyinbo <i>et al.</i> , 2017)
Gabon	<i>mab</i>	10	10	(Bastin <i>et al.</i> , 2015; Labrière <i>et al.</i> , 2018)
South America				
Peru	<i>tam</i>	6	6	https://www.forestplots.net/en/ (Boyd <i>et al.</i> , 2013)
Brazil	<i>s11</i>	9	1.44	http://www.paisagenslidar.cnptia.embrapa.br/webgis/
Brazil	<i>s12</i>	19	4.8	http://www.paisagenslidar.cnptia.embrapa.br/webgis/
Central America				
Costa Rica	<i>lsv</i>	12	6	https://tropicalstudies.org/carbono-project/
Costa Rica	<i>cha</i>	3	2	
Panama	<i>bci</i>	1	50	https://forestgeo.si.edu/sites/neotropics/barro-colorado-island (Lobo & Dalling, 2013)

156 In this study, we assessed the structure-richness relationship at three spatial resolutions (1.0, 0.25,
 157 0.0625 ha) because of the non-linear relationship between the number of tree species (S) and sampled
 158 area. We selected squares of 1.0 ha (100x100 m) because they are often-used in ecology and it has been
 159 shown that the spatial mismatch of plot location and remote sensing products is minimized at this
 160 resolution (Réjou-Méchain *et al.*, 2014). We used squares of 0.25 ha (50x50 m) because these yielded
 161 the best results describing the structure-diversity relationship in Gabon (Marselis *et al.*, 2019), and
 162 squares of 0.0625 ha (25x25 m) because they correspond to a resolution close to the GEDI footprint size.
 163 The datasets were used at one, two or three of the aforementioned resolutions depending on the
 164 original plot size and the availability of stem maps or subplots (**Error! Reference source not found.**, full

165 table in SI1). For each of the field sites we calculated S for the entire dataset and for each plot at each
 166 plot size (Table 2). Only live trees with a DBH ≥ 10 cm were included, to ensure consistency among
 167 datasets and we removed all plots of each resolution in which more than 20% of the trees were not
 168 identified to the genus level.

169 *Table 2: The total number of species identified at each study site and the average (\bar{x}) and standard*
 170 *deviation (s) of the species richness for each of the three plot sizes expressed as $\bar{x} \pm s$ (including only live*
 171 *trees with DBH ≥ 10 cm).*

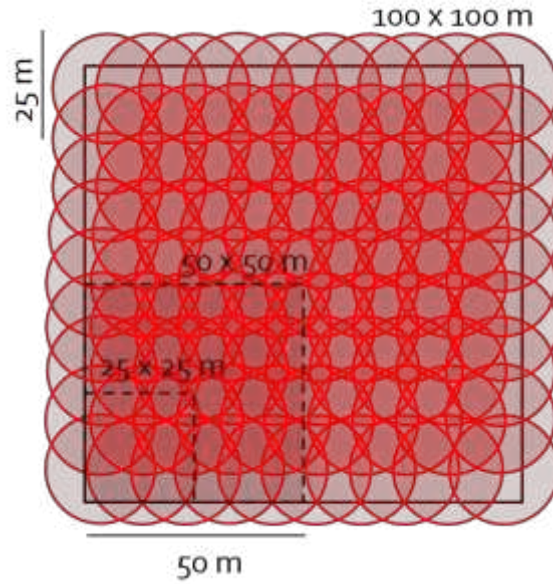
Country	Project Name	Total No. species	Total sampled area used (ha)	Species richness 1.0 ha	Species richness 0.25 ha	Species richness 0.0625 ha
<i>Oceania</i>						
Australia	<i>rob</i>	205	25	98 \pm 10	56 \pm 8	27 \pm 5
<i>South-East Asia</i>						
Malaysia	<i>dan</i>	430	2	117 \pm 13	51 \pm 7	19 \pm 4
Malaysia	<i>sep</i>	517	32	102 \pm 22	53 \pm 11	-
<i>Africa</i>						
DRC	<i>mal</i>	116	21	37 \pm 11	20 \pm 7	-
DRC	<i>yan</i>	232	9	50 \pm 23	24 \pm 13	10 \pm 6
Gabon	<i>rab</i>	234	25	84 \pm 8	42 \pm 6	17 \pm 4
Gabon	<i>lop</i>	118	9.5	32 \pm 22	17 \pm 10	8 \pm 4
Gabon	<i>mon</i>	146	10	32 \pm 15	15 \pm 9	7 \pm 5
Gabon	<i>mab</i>	196	10	55 \pm 8	-	-
<i>South America</i>						
Peru	<i>tam</i>	517	6	171 \pm 13	70 \pm 9	24 \pm 5
Brazil	<i>s11</i>	91	1.44	-	-	17 \pm 3
Brazil	<i>s12</i>	135	4.8	-	-	16 \pm 4
<i>Central America</i>						
Costa Rica	<i>lsv</i>	216	6	-	48 \pm 8	19 \pm 5
Costa Rica	<i>cha</i>	81	2	58	28 \pm 5	13 \pm 4
Panama	<i>bci</i>	220	50	87 \pm 8	42 \pm 6	17 \pm 3

172

173 2.2 Lidar Datasets

174 Each of the field datasets had coincident discrete return airborne laser scanning (ALS) data, or full-
 175 waveform lidar data from the Land Vegetation and Ice Sensor (LVIS), collected over the field plots within
 176 5 years of field data collection. We used the GEDI simulator (Hancock *et al.*, 2019) to create lidar
 177 waveforms from the ALS data over the field plots. The ALS data was originally collected with a variety of

178 airborne instruments, but the GEDI simulator ensures a reliable GEDI-like waveform with minimal
179 influence of the original instrument-specific characteristics. In this way, all lidar information could be
180 processed in a consistent way across all study sites ensuring a reliable inter-comparison of canopy
181 structure metrics derived from the waveforms and allowing for easy transfer of the developed models to
182 future on-orbit GEDI data. Lidar waveforms were simulated with a 22 m ground footprint (Gaussian
183 distribution of laser energy, $\sigma = 5.5$ m). Lidar waveform locations were determined by filling each field
184 plot, using the original field plot size and shape, with footprint center locations 6.25 m from the plot
185 edge and 5 m between footprint center locations (**Error! Reference source not found.**). In this way, a
186 reliable measure of canopy structure could be acquired for each plot by averaging lidar metrics from all
187 waveforms inside the plot, instead of using single waveforms in the plot center and evaluating structure-
188 richness relationships based on such potentially biased or unrepresentative waveforms. The following
189 information was extracted from each simulated lidar waveform using mature and published algorithms:
190 canopy height (expressed as the 98th percentile of the relative height metric; RH98), total Plant Area
191 Index (PAI), and Plant Area Index at a 1 m vertical resolution (Drake *et al.*, 2002; Tang *et al.*, 2012;
192 Marselis *et al.*, 2018; Hancock *et al.*, 2019). The 1 m vertical profile was used to compare the canopy
193 structure across the study sites. It was aggregated into a 10 m vertical profile, summing all PAI values in
194 each 10 m vertical bin, to be used in the structure-richness analyses. We chose to use the PAI profile
195 because it is a biophysical variable describing the amount of plant material along the vertical forest axis,
196 thus directly indicating the occupation of vertical niche space, and Marselis *et al.*, (2019) previously
197 showed this information relates well to tree species richness in Africa. The average of each of the
198 resulting metrics from all waveforms within each plot was computed to represent the canopy structure
199 for each plot at each spatial resolution.



200
 201 *Figure 2: Illustration of simulated lidar waveform layout. The waveforms (red circles) have a Gaussian*
 202 *energy distribution with $\sigma=5.5$ m, resulting in a roughly 22 m diameter footprint. Example of simulated*
 203 *footprint distribution locations in a 1.0 (solid outline), 0.25 and 0.0625 ha field plot (dashed outline).*

204 **2.3 Canopy Structure across the tropics**

205 To evaluate the canopy characteristics across the different study sites we calculated the median plant
 206 area volume density profile (composed of the PAI values for each 1 m vertical bin), using all simulated
 207 lidar waveforms for each study site. In addition to the median (50th percentile), we calculated the 10, 30,
 208 70 and 90th percentiles of the PAI values in the same 1 m vertical bins, to provide a representative
 209 distribution of the canopy structure across the study site.

210 **2.4 Species-area relationships across the tropics**

211 We created species-area relationships, calculating the mean and standard deviation of S for plot sizes
 212 ranging between 0.01 and 50 ha, to assess how species richness changes by plot size across our study
 213 sites. Each of the original field plots was filled with as many non-overlapping subplots as possible at 17
 214 spatial resolutions (0.01, 0.0225, 0.04, 0.09, 0.16, 0.25, 0.36, 0.64, 1.0, 2.25, 4.00, 6.25, 9.00, 12.25, 16.0,
 215 25.0, 50.0 ha) with each tree assigned to a subplot at each resolution. The plot sizes used at each study
 216 site depended on the original plot size and the availability of stem maps (SI1). We visualized the mean

217 and standard deviation of S for each plot size at each study site to evaluate the differences in species-
218 area curves across the tropics.

219 **2.5 Structure-Richness Analysis**

220 To evaluate the existence of a relationship between vertical canopy structure and tree species richness
221 across the tropics, we developed models at three scales: local, regional and pan-tropical, because many
222 historical and environmental drivers of (tree) species diversity have stronger or weaker relations
223 depending on the scale of observation (Gaston, 2000; Keil & Chase, 2019) as do different ecosystem
224 functions (Chisholm *et al.*, 2013). Definitions of the scales are presented in the following sections.

225 **2.5.1 Local Analysis**

226 The local analysis focused on the structure-richness relationship within large (25 or 50 ha) plots. We
227 used data from adjacent field plots to evaluate the relationship between S and the canopy structure
228 expressed as canopy height (RH98), total PAI and vertical canopy profile (PAI at 10 m vertical intervals).
229 The local analysis was performed on data collected in *bci* (50 ha), *rab* and *rob* (25 ha). The other 50 ha
230 plot (*dan*) was not suitable for this analysis because the species identification was incomplete at the
231 time of analysis (**Error! Reference source not found.**, **Error! Reference source not found.**). We related
232 the canopy structure with S using a generalized linear model with a Poisson error distribution. We used
233 5-fold cross-validation, extracting 20% of the data at random in each fold as test data. We first
234 performed feature selection on the training data, choosing the model with the lowest Bayesian
235 Information Criterion (BIC) score, and then constructed the predictive model based on the same training
236 data. We evaluated model performance using R^2 , Root Mean Squared Difference as a percentage of the
237 mean (RMSD%) and bias based on the predictions for the test data (Piñeiro *et al.*, 2008). The average
238 and 95% confidence interval of these metrics were recorded for each study site at each resolution.

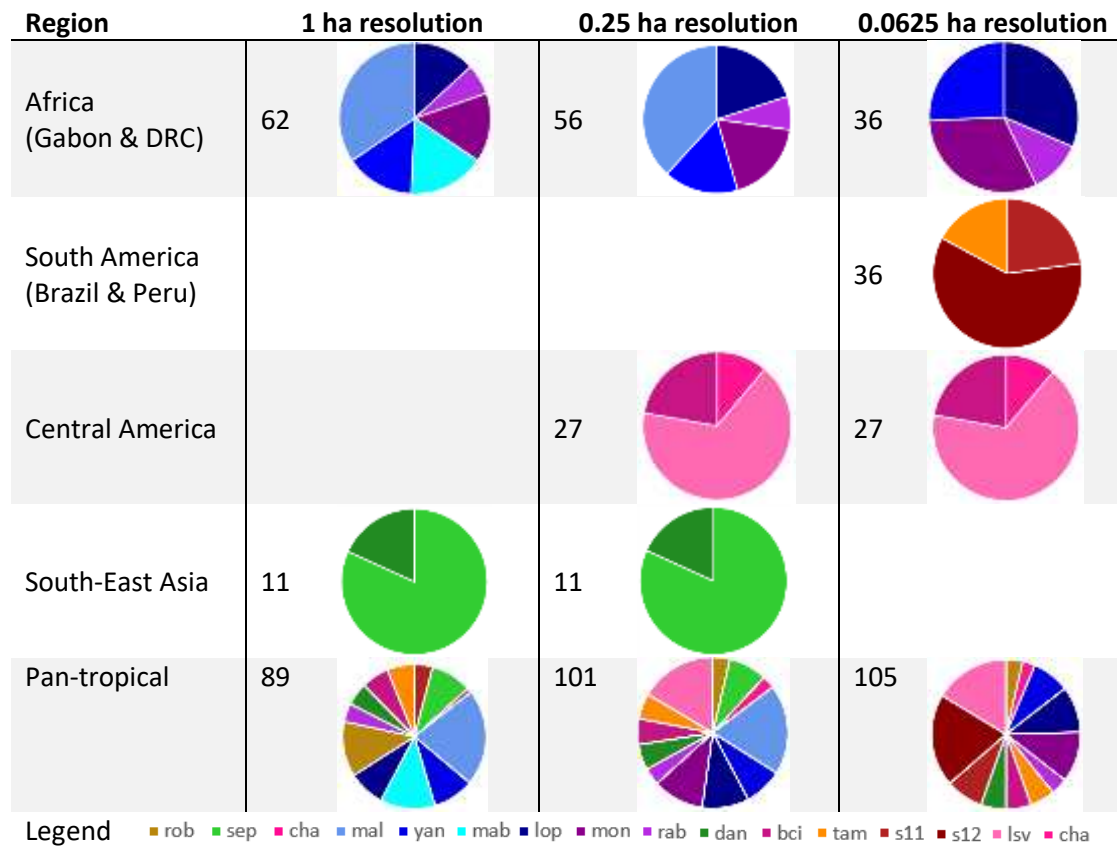
239

240 2.5.2 Regional and Pan-tropical Analysis

241 The regional analysis was focused on the structure-richness relationship based on non-adjacent plots
242 across study sites within the same biogeographical zone. We evaluated different combinations of study
243 sites at three spatial resolutions (**Error! Reference source not found.**). To prevent the large plots from
244 dominating the regional and pan-tropical analyses, we thinned their contribution to both the regional
245 and pan-tropical datasets. From the 25 ha plots we selected 1.0 ha plots at each corner, and from the 50
246 ha plots we selected all corner and the middle plots along the long sides of the plot (6 1.0 ha plots total).
247 To avoid mixing local and regional effects, we employed a Monte-Carlo simulation approach in which we
248 drew different samples from the full regional dataset. In each Monte-Carlo run we randomly sampled
249 one plot at the given resolution from each original plot location (especially important at the 0.25 and
250 0.0625 ha resolutions at which up to 16 plots exist at the location of each original 1.0 ha plot) and
251 applied a cross-validation (80/20) or leave-one-out cross validation (if $n \leq 25$) approach. In the cross-
252 validation we again performed a two-step approach: first we performed variable selection on the
253 Poisson regression model choosing the model with lowest BIC (using the *bestglm* package in R), and
254 then built the predictive model with the chosen variables. We applied the model to the test data and
255 calculated the model performance statistics for each fold according to Piñeiro *et al.* (2008).

256 The pan-tropical analysis focused on the structure-richness relationship combining the information from
257 all 15 study sites across all tropical regions, in other words, it was a special case of the regional analysis
258 in which data from all sites was included. Thus applying the same methods as for the regional analysis.

259 *Table 3: Datasets used for regional and pan-tropical analysis of the structure-richness relationships. Note*
 260 *that one region may not contain the same number of plots across all resolutions (values in the table*
 261 *indicate total number of plots for each region) and resolution due to limitations in the availability of*
 262 *subplot and stem map information, limiting the use of data from some study sites to only one or two*
 263 *resolutions.*

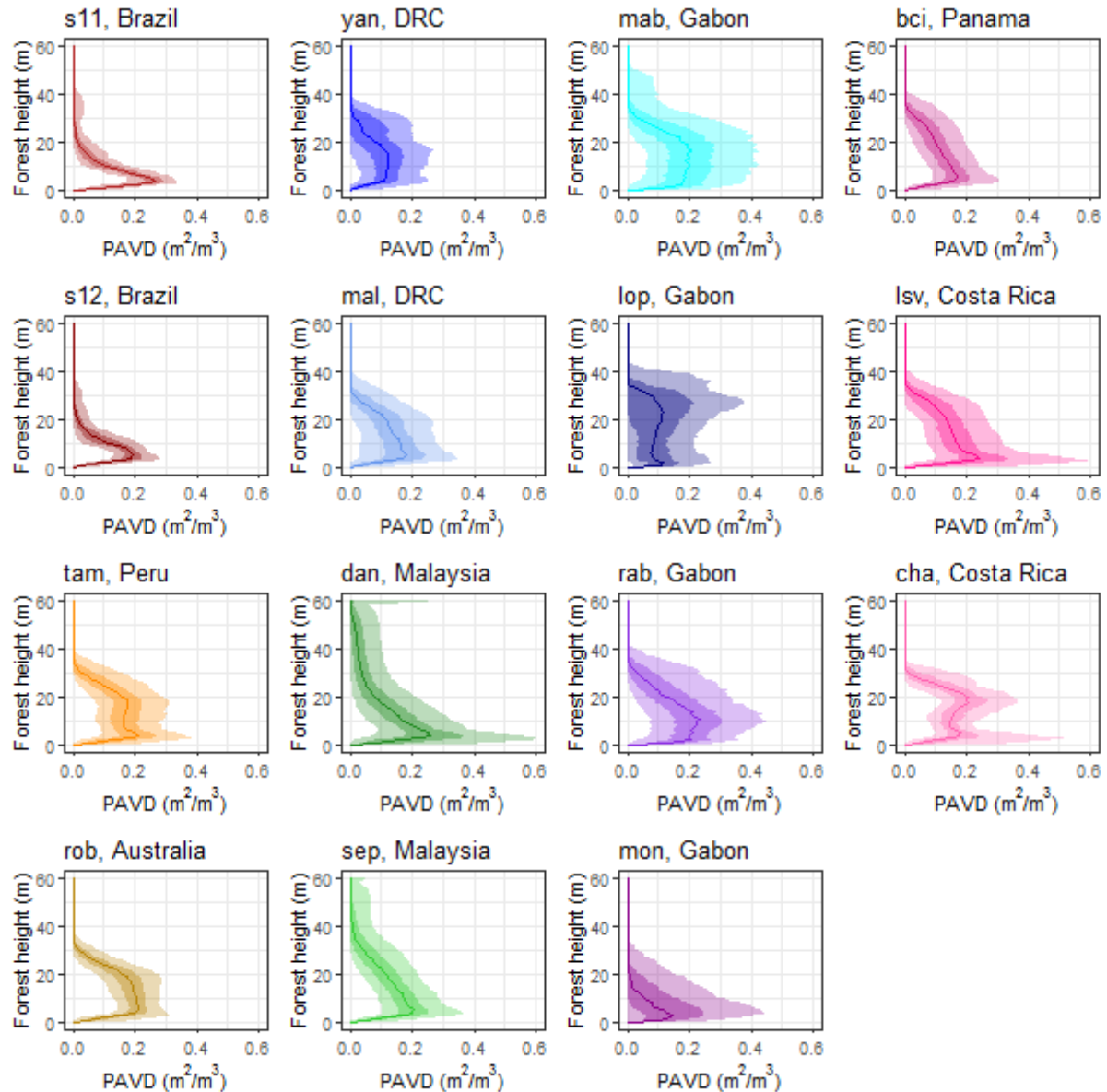


264

265 **3. Results**

266 **3.1 Vertical forest structure across the tropics**

267 The vertical canopy structure of forests, in terms of the vertical distribution of plant material varies
268 between tropical regions (**Error! Reference source not found.**). Maximum canopy height in our study
269 sites in the Neotropics and Central Africa is typically around 40 m, and slightly lower in Australia, while
270 canopy heights in South-East Asia exceed 60 m. Many sites show a distinct understory layer and a
271 decrease in plant material through the canopy. Relative to the understory, the canopy layer sharply
272 declines in vegetation density (*sep* and *dan*, Malaysia) or steadily declines along the vertical axis (*bci*,
273 Panama; *rab*, Gabon; *mal*, DRC; *rob*, Australia). This vertical distribution of declining vegetation is
274 exacerbated in degraded forests: in *s11*, *s12* (Brazil) and *mon* (Gabon), where the bulk of the vegetation
275 exists close to the forest floor at ~5 m height, but remnant trees in some plots may reach 40 m. Other
276 sites, especially undisturbed ones, have distinct canopy layers. In *tam* (Peru) and in the old-growth
277 forest in *lsv* (Costa Rica) there are multiple peaks of high-density vegetation across the vertical strata of
278 the forest. The profiles of *yan* (DRC) and *lop* (Gabon) are characterized by a multiple-peak pattern, with
279 one peak 20-30 m in the canopy and another within 5 m of the ground, reflecting the inherent structure
280 of the forest-savanna mosaic. The less disturbed *mab* (Gabon) forest shows high variability in canopy
281 structure between plots (e.g. the wide shaded area in Figure 3) and higher canopies.



282
 283 *Figure 3: Canopy structure expressed as the Plant Area Volume Density profile (PAVD), expressing the*
 284 *Plant Area Index for each 1 m vertical bin, displayed as the median of all plots within each study site*
 285 *(solid line), the 30th-70th percentile (darker shaded area) and 10th-90th percentile (lighter shaded area).*

286

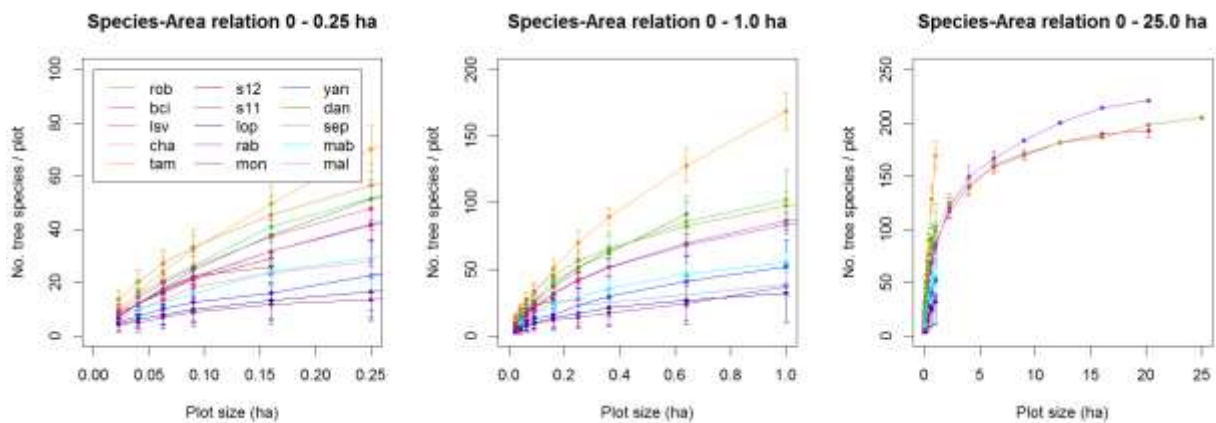
287 3.2 Species-area relationships

288 The number of species increases with plot size, but the rate of increase varies across study sites (**Error!**

289 **Reference source not found.**). For example, in *rob* (Australia) 82-117 species occur in a 1.0 ha plot

290 compared to 16-44 species in 0.0625 ha plots. By contrast, *tam* (Peru) contains 154-185 species/ha, but

291 only 11-35 species in a 0.0625 ha plot, similar to *rob*. Thus, species' composition of adjacent 0.0625 ha
 292 plots in *tam* must be more different from each other than adjacent 0.0625 ha plots in *rob* (Australia), in
 293 other words, the β diversity of the plots in *tam* is higher than in *rob*. The species-area curves vary in
 294 shape across study sites, with the highest total species richness in *tam* and lowest species richness in the
 295 African sites (**Error! Reference source not found.**). Curves that are initially steep and decrease in slope
 296 at larger plot sizes indicate a high α diversity but a lower β diversity (e.g. when the area is increased, the
 297 same species are encountered).

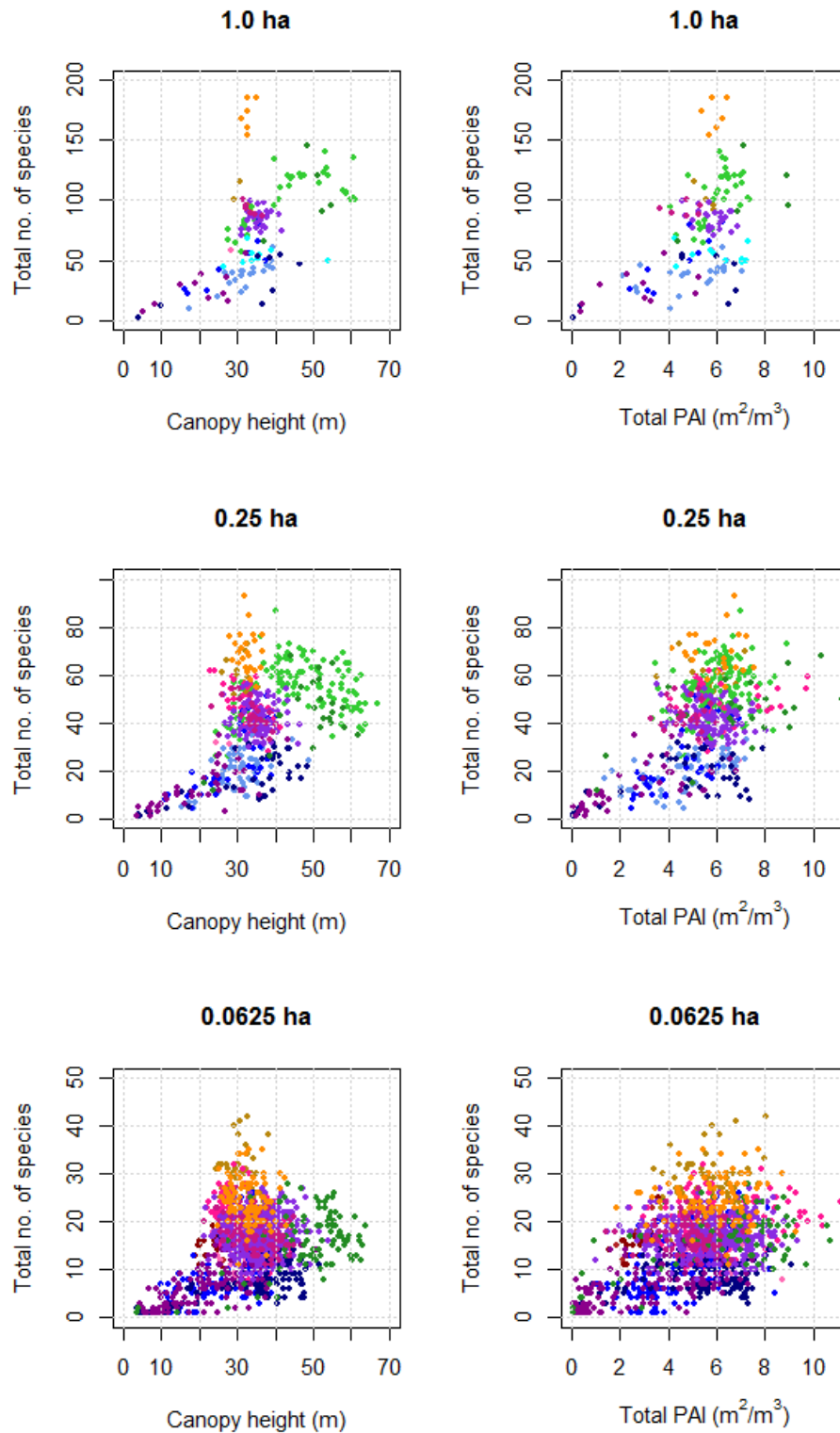


298
 299 *Figure 4: Relationships between tree species richness and area for each study site (note the change in y-*
 300 *axis across panels from left to right).*

301

302 3.3 Structure-richness relationships

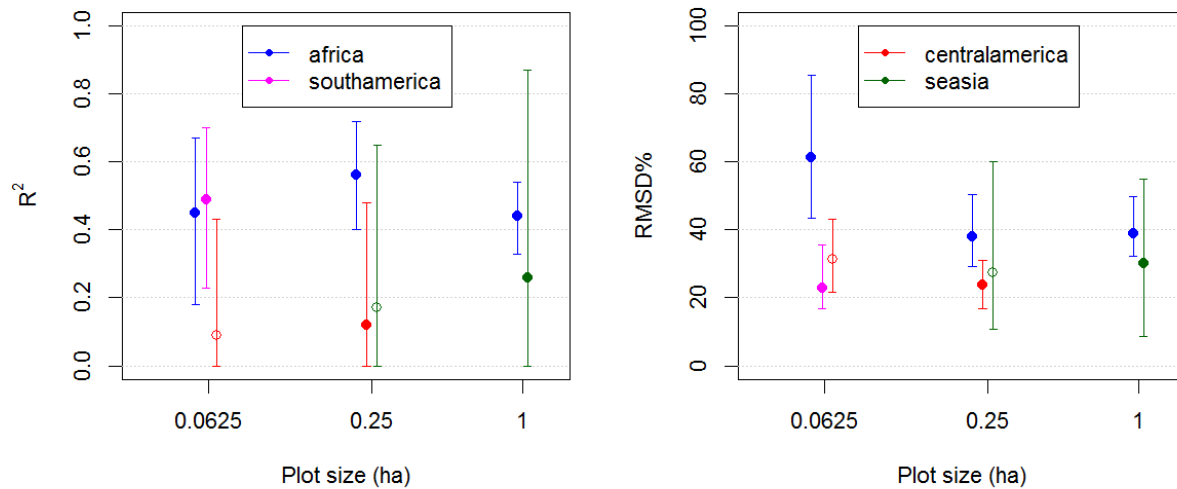
303 Pulling together the information on tree species richness and canopy structure (RH98 and Total PAI),
 304 species richness generally increases with increasing canopy height and increasing total Plant Area Index
 305 across the tropics (Figure 5).



306
 307 *Figure 5: Relation between canopy height (left) and total PAI (right) across three spatial scales for all*
 308 *study sites across the tropics. Each point represents one plot at the specific resolution. Dots are colored*
 309 *by study site corresponding to legend in Figure 1.*

310 The cross-validation results of the local models reveal weak structure-richness relationships. Of the
311 three large plots (25 and 50 ha), only the models for *bci* (50 ha) show evidence of a significant
312 relationship between the predicted and observed values ($R^2=0.32$ at 1.0 ha, SI2). Even though species
313 richness within all three large plots can be predicted with a root mean squared error between 7-20% of
314 the mean species richness, the low RMSD% found only indicates that the predictions at the local scale
315 are close to the mean species richness, however in *rab* and *rob* the canopy structure is insensitive to the
316 local variation in tree species richness (see example figure in SI2).

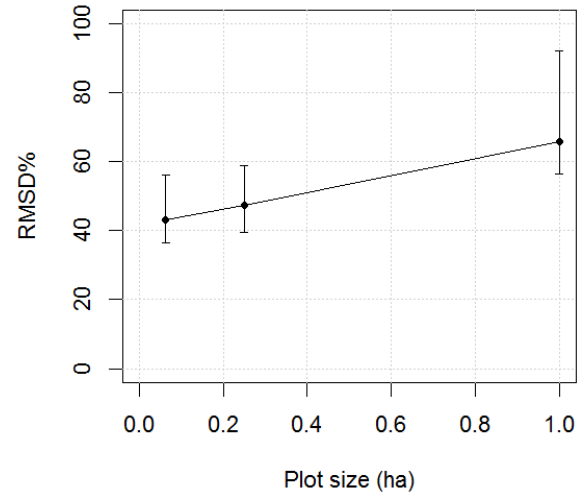
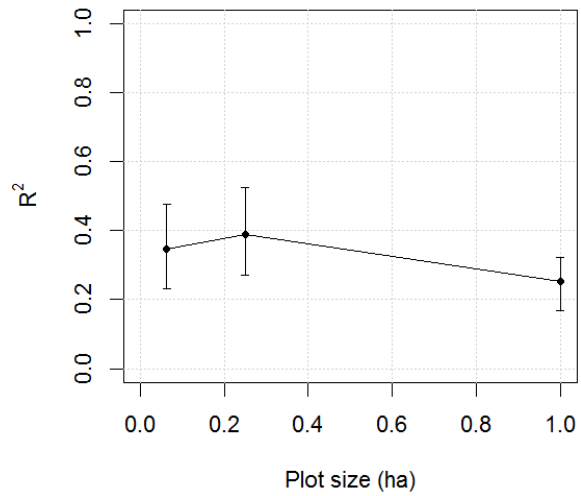
317 Regional structure-richness models generally show much better performance (Figure 6) than the local
318 models in terms of the variance in species richness that can be explained with the canopy structure
319 information (mostly significant models and higher R^2 values). However, prediction error (as percentage
320 of the mean species richness) is generally higher, partly due to the larger range in species richness in
321 these regional datasets. Regions of Africa and South America (Table 3) show the best model
322 performance whereas regions including the Costa Rica datasets show much poorer performance
323 (regions indicated with *centralamerica*). Results from an additional analysis on the compositional
324 similarity (Bray-Curtis; Faith *et al.*, 1987, SI3) of the Costa Rica dataset showed that, even though species
325 richness varies in Costa Rica (**Error! Reference source not found.**), the plots share many species, i.e. the
326 composition is similar. In the *africa* and *southamerica* datasets the variation in species richness is
327 accompanied by a much larger variation in species composition (SI3). The variation of the model
328 performance for *seasia* is very high to the low number of plots available for this region and at the 0.25
329 ha resolution it was not possible to create a significant model >95% of the monte-carlo iterations (Table
330 3).



331 *Figure 6: Cross-validated model performance of regional structure-richness models. Error bars indicate*
 332 *the 95% range of values for each performance metric. Solid dots indicate >95% of the generated models*
 333 *was statistically significant, open circles indicate a lower percentage was significant.*
 334

335 Pan-tropical structure-richness models show more similar performance across all spatial resolutions
 336 with mean R² ranging between 0.25 and 0.39 and RMSD% between 66 and 43%, for the plot sizes from
 337 1.0 and 0.0625 ha (Figure 8), indicating that around 39% of the variation in tree species richness can be
 338 explained using canopy structure metrics alone at the 0.25 ha resolution at the global scale. Sites with
 339 extremely high values of observed species richness are generally predicted poorly (SI4).

340



341

342 *Figure 7: Cross-validated model performance at the pan-tropical scale in terms of R^2 and RMSD%. Error*
 343 *bars indicate the range between which 95% of the performance values of the cross-validated models fall.*

344

345 **4. Discussion**

346 **4.1 Structure-richness relationships across scales**

347 In this study we explored the relationships between vertical canopy structure and tree species richness
348 at different resolutions across local, regional and pan-tropical scales. We found weak relationships
349 between canopy structure and tree species richness at the local scale and the strongest relationship at
350 the regional scales in Africa and South America. We also found significant relationships between canopy
351 structure and tree species richness combining the data from all study sites across the tropics.

352 At the local scale, within one big plot inside one forest type, the variation in the canopy structure is
353 determined largely by variability in growth structure within the same species (the 25 and 50 ha plots
354 have a similar composition throughout the plot, SI1). For example, an adult tree of species X may range
355 in height from 20-40 m, so even though structure may differ between two plots of similar composition,
356 the difference is not attributed to a difference in species composition. Furthermore, if a 20 m and 40 m
357 tree of species X exist in the same plot, due to the difference in canopy structure the model may predict
358 a species richness of 2 based on variation in structure. On the other hand, as area increases it is more
359 likely that the difference in structure is caused by a difference in composition. Individuals of most
360 tropical forest species are spatially aggregated (Condit, 2000) so the composition of two adjacent plots is
361 more similar than the composition of two more distant plots. This is the case for *bci*, where a 50 ha area
362 was sampled and included in the local analysis, which led to more successful prediction of species
363 richness based on structure. Within the 25 ha plots sampled at *rab* and *rob*, the variation in composition
364 is smaller and no significant structure-richness relationships were found (SI3).

365 Increasing the scale, we found that regions consisting of sites exhibiting a large variation in species
366 composition among plots, but with a similar biogeographical history, show a much stronger structure-
367 richness relationship. However, we note that model performance differed quite drastically across

368 regions. The forest in *lsv*, Costa Rica, consists of largely similar species composition, whereas species
369 composition is much more different in regions where the structure-richness models perform better
370 (South-America, Africa), supporting the result from local scale models that species richness can be
371 better predicted from canopy structure in areas with greater β diversity.

372 At the pan-tropical scale we find a significant relationship between canopy structure and tree species
373 richness across all spatial resolutions. At the intermediate resolution (0.25 ha) this relationship appears
374 to be slightly stronger than at the higher and lower resolutions, but no significant difference was found.
375 However, the observed difference may be attributed to the lower sensitivity of species richness to rare
376 species at smaller plot sizes. For example, *tam* (Peru) plots have very high species richness at the 1.0 ha
377 resolution (**Error! Reference source not found.**), whereas at the 0.0625 ha resolution the species
378 richness ranges between 11-35 species, which is still higher than most other sites but much less than at
379 the 1.0 ha plot size. Because the 1.0 ha plot size captures more rare species in each plot, the 1.0 ha pan-
380 tropical model predictions for *tam* contain highly erroneous predictions that are not present in 0.0625
381 ha models (SI4). Rare species do not contribute much to the canopy structure, thereby complicating the
382 relationship between structure and richness at a scale at which they contribute largely to species
383 richness numbers.

384 **4.2 Limitations**

385 This research could be significantly improved by using more coincident lidar and field data to thoroughly
386 evaluate the existence and strength of the structure-richness relationship across all tropical regions.
387 However, the collection of such data is costly and time-consuming. Here, we were able to exploit 15
388 independently collected datasets (SI1). However, there is quite a data gap, especially in the Amazon
389 basin, the mainland of South-East Asia, New Guinea and Australia. Apart from the spatial representation
390 problem, the low number of plots for certain regions attributes largely to the observed variability in

391 model performance. The pan-tropical models (with $n \geq 89$) show much more stable performance than
392 models of regions with low numbers of plots (e.g. *seasia*). A training dataset that does not fully
393 represent the range of structure in the full dataset can lead to highly erroneous predictions for some of
394 the test plots. Such errors are exacerbated by the logarithmic link model in Poisson regression because
395 errors can increase exponentially. Even so, negative predictions are possible with linear regression and
396 the risk of underestimating tree species richness is higher for diverse areas. Hence, we chose to use
397 Poisson regression, knowing that it may lead to extreme predictions in some cases that should be
398 accounted for when operationalizing this method.

399 Species diversity can be identified in many different ways (Gotelli & Colwell, 2001; Colwell, 2009) and
400 there are risks and pitfalls using just one metric. In this study we only used 'species richness' (S), defined
401 by the number of different tree species in a defined area (the plot, with different sizes), as this metric is
402 easy to interpret and a prediction of the number of species/area can probably be used most directly by
403 ecosystem managers. Hereby we did not control for the number of stems in the plot, nor for the
404 abundancy of the different species. Such things can be taken into account for example by using the
405 Shannon diversity index or rarefaction curves. Moreover, depending on the type of metric, a different
406 model will need to be selected. For example, a generalized linear regression with a Poisson error
407 distribution, as used here, is more suitable for estimated tree species richness as this is count data,
408 whereas a linear model with a Gaussian error distribution will be better for estimating Shannon
409 diversity. Hence, we chose to focus on one metric of diversity to test the structure-richness
410 relationships, while acknowledging other metrics may provide better, worse, or more useful predictions
411 of tree species diversity and these should be considered in the future.

412 This study serves as a first attempt to study the pan-tropical structure-richness relationship and should
413 be improved and further developed when more data become available. Additionally, the characteristics
414 of each dataset differed widely because all data were collected by different people and institutions. We

415 accounted for this as much as possible by using datasets only at reliable plot and subplot resolutions,
416 including only trees ≥ 10 cm DBH and including only plots with less than 20% of unidentified trees at the
417 genus level. Nonetheless, we acknowledge that the quality of the species identification varied and may
418 have affected our models as species identification in the tropics can be challenging due to the vast
419 variety of tree species and the fact that new species are still encountered. Species identification of new
420 and existing data could be improved using more botanists or genetic tests in the lab, which has been
421 done for some of the datasets used here, but is not yet feasible for all datasets.

422 The availability of stem maps and subplots in each study site determined the spatial resolutions at which
423 datasets could be used. This resulted in the inclusion of different datasets for each region (Table 3). This
424 makes the comparison of model performance in the same region at different resolutions unreliable
425 because the models were not always built on the same data (plots and study sites), but we weighed this
426 decision to maximize the sizes of the datasets used to build the structure-richness models. Hence, no
427 conclusion can be drawn about the optimal resolution for the structure-richness relationships.

428 Accurate geolocation of field plots is key for the development of reliable species-richness models.
429 However, geolocation of field plots in the tropical forest can be challenging due to difficulties receiving a
430 reliable GPS signal under dense canopy. This should be taken into account, especially when evaluating
431 the performance of models build with small field plots, where the effects of such geolocation errors will
432 be larger (Réjou-Méchain *et al.*, 2014).

433 We included data from a range of forest stages, including old-growth forest, successional stages,
434 disturbed forest and even low tree density savanna sites. The relationships we found are partially driven
435 by this gradient (Figure 5). However, we deemed it essential to include data from across this range of
436 forest types, because if this method is to be operationalized using canopy structure information from
437 across the tropics, we will encounter all these different stages of forest (Lewis *et al.*, 2015).

438 4.3 Future research & Applications

439 Our results provide confidence regarding the existence of regional and pan-tropical structure-richness
440 relationships that may be used to map pan-tropical tree species richness. The most accurate predictions
441 seem to be achieved at the regional scale when adequate data are available and when forested areas
442 are grouped by regions of similar biogeographical history. However, in the absence of such data it may
443 be of more immediate interest to further develop pan-tropical models that can explain up to 39% of
444 variation in tree species richness. At the time of writing, GEDI is collecting canopy structure information
445 close to the finest resolution tested here (0.0625 ha) and thus these data may be well suited for
446 mapping tree species richness across the tropics. GEDI is a sampling mission in which lidar waveforms
447 with 25 m diameter footprints are collected across 8 tracks (600 m between-track spacing, 60 m along-
448 track spacing). GEDI gridded data products will have a 1 km² resolution in which the GEDI data samples
449 are averaged to 1 km² values (Dubayah *et al. under review*). Our local scale models show that
450 predictions of adjacent 0.0625 ha plots (or in the future, footprints) are on average correct, but they will
451 not detect local nuances in species richness within forests of uniform composition. We suggest that the
452 species richness predictions could potentially be used in a similar way as for gridded GEDI data products
453 and estimate the average number of species/0.0625 ha within a 1 km² cell, as such information may still
454 be of interest to local land managers. Given the variable species-area relationships, it is not easy to
455 translate species richness predictions at 0.0625 ha resolution to the expected number of tree species in
456 1 km². Also, the amount of variance in species richness explained is limited. Therefore, we propose two
457 future research avenues of interest: fusion with spectral and/or radar data and using an environmental
458 framework. Both spectral data and radar data have previously been shown to predict some of the
459 variance in tree species richness (Foody & Cutler, 2006; Wolf *et al.*, 2012; Schäfer *et al.*, 2016; Bae *et al.*,
460 2019; Bongalov *et al.*, 2019; Marselis *et al.*, 2019) and may improve our models and allow for more
461 accurate predictions of tree species richness across the tropics and the creation of wall-to-wall data

462 products at higher spatial resolution. Especially data from the hyperspectral HISUI (Matsunaga *et al.*,
463 2013) instrument, that is soon to be launched to the International Space Station, the radar BIOMASS
464 mission (Le Toan *et al.*, 2011), or the TanDEM-X mission (Qi *et al.*, 2019), may be highly relevant for such
465 applications. Alternatively, we believe that the inclusion of structural data within previously developed
466 environment and biogeographical frameworks will help to predict tree species diversity (Keil & Chase,
467 2019). Such frameworks could benefit from GEDI lidar data providing information on the occupation of
468 the vertical niche space and likely improve predictions of tree species richness across the tropics.

469 **5. Conclusions**

470 In this study we evaluated the existence of local, regional and pan-tropical relationships between
471 vertical canopy structure and tree species richness in the tropics at three spatial resolutions: 1.0, 0.25,
472 and 0.0625 ha. Our results show that canopy structure can explain a limited percentage of variation in
473 tree species richness across the different regions. On a pan-tropical scale, 39% of the variation in tree
474 species richness can be explained with the vertical canopy structure using one single predictive model at
475 a 0.25 ha plot size. A full set of regional structure-richness models will most likely aid accurate pan-
476 tropical species richness mapping, but the development of such a set of models is contingent on the
477 availability of sufficient coincident field & lidar data across the tropics. Alternatively, canopy structure
478 information from GEDI could be included in existing modeling frameworks, combining spectral,
479 environmental and structural information to provide more accurate tree species richness predictions.

480 References

- 481 Bae, S., Levick, S.R., Heidrich, L., Magdon, P., Leutner, B.F., Wollauer, S., Serebryanyk, A., Nauss, T.,
482 Krzystek, P., Gossner, M.M., Schall, P., Heibl, C., Bassler, C., Doerfler, I., Schulze, E., Krah, F.,
483 Culmsee, H., Jung, K., Heurich, M., Fischer, M., Seibold, S., Thorn, S., Gerlach, T., Hothorn, T.,
484 Weisser, W.W. & Muller, J. (2019) Radar vision in the mapping of forest biodiversity from space.
485 *Nature Communications*, **10**, 4757.
- 486 Bastin, J.F., Barbier, N., Réjou-Méchain, M., Fayolle, A., Gourlet-Fleury, S., Maniatis, D., De Haulleville, T.,
487 Baya, F., Beeckman, H., Beina, D., Couteron, P., Chuyong, G., Dauby, G., Doucet, J.L., Droissart, V.,
488 Dufréne, M., Ewango, C., Gillet, J.F., Gonmadje, C.H., Hart, T., Kvali, T., Kenfack, D., Libalah, M.,
489 Malhi, Y., Makana, J.R., Pélissier, R., Ploton, P., Serckx, A., Sonké, B., Stevart, T., Thomas, D.W., De
490 Cannière, C. & Bogaert, J. (2015) Seeing Central African forests through their largest trees. *Scientific*
491 *Reports*, **5**.
- 492 Bongalov, B., Burslem, D.F.R.P., Jucker, T., Thompson, S.E.D., Rosindell, J., Swinfield, T., Nilus, R.,
493 Clewley, D., Phillips, O.L. & Coomes, D.A. (2019) Reconciling the contribution of environmental and
494 stochastic structuring of tropical forest diversity through the lens of imaging spectroscopy. *Ecology*
495 *Letters*, **22**, 1608–1619.
- 496 Boyd, D.S., Hill, R.A., Hopkinson, C. & Baker, T.R. (2013) Landscape-scale forest disturbance regimes in
497 southern Peruvian Amazonia. *Ecological Applications*, **23**, 1588–1602.
- 498 Bradford, M.G., Metcalfe, D.J., Ford, A., Liddell, M.J. & McKeown, A. (2014) Floristics, stand structure
499 and aboveground biomass of a 25-ha rainforest plot in the wet tropics of Australia. *Journal of*
500 *Tropical Forest Science*, **26**, 543–553.
- 501 Carlson, K.M., Asner, G.P., Hughes, R.F., Ostertag, R. & Martin, R.E. (2007) Hyperspectral remote sensing
502 of canopy biodiversity in Hawaiian lowland rainforests. *Ecosystems*, **10**, 536–549.
- 503 Chisholm, R.A., Muller-Landau, H.C., Abdul Rahman, K., Bebbler, D.P., Bin, Y., Bohlman, S.A., Bourg, N.A.,
504 Brinks, J., Bunyavejchewin, S., Butt, N., Cao, H., Cao, M., Cárdenas, D., Chang, L.W., Chiang, J.M.,
505 Chuyong, G., Condit, R., Dattaraja, H.S., Davies, S., Duque, A., Fletcher, C., Gunatilleke, N.,
506 Gunatilleke, S., Hao, Z., Harrison, R.D., Howe, R., Hsieh, C.F., Hubbell, S.P., Itoh, A., Kenfack, D.,
507 Kiratiprayoon, S., Larson, A.J., Lian, J., Lin, D., Liu, H., Lutz, J.A., Ma, K., Malhi, Y., McMahon, S.,
508 Mcshea, W., Meegaskumbura, M., Mohd. Razman, S., Morecroft, M.D., Nytch, C.J., Oliveira, A.,
509 Parker, G.G., Pulla, S., Punchi-Manage, R., Romero-Saltos, H., Sang, W., Schurman, J., Su, S.H.,
510 Sukumar, R., Sun, I.F., Suresh, H.S., Tan, S., Thomas, D., Thomas, S., Thompson, J., Valencia, R.,
511 Wolf, A., Yap, S., Ye, W., Yuan, Z. & Zimmerman, J.K. (2013) Scale-dependent relationships between
512 tree species richness and ecosystem function in forests. *Journal of Ecology*, **101**, 1214–1224.
- 513 Colwell, R.K. (2009) *Biodiversity: concepts, patterns and measurement. The Princeton guide to ecology*,
514 pp. 257–263.
- 515 Condit, R. (2000) Spatial patterns in the distribution of tropical tree species. *Science*, **288**, 1414–1418.

516 Corlett, R.T. & Primack, R.B. (2011) *Tropical Rain Forests: An Ecological and Biogeographical*
517 *Comparison: Second Edition*, 2nd edn. Blackwell Publishing.

518 Drake, J.B., Dubayah, R.O., Knox, R.G., Clark, D.B. & Blair, J.B. (2002) Sensitivity of large-footprint lidar to
519 canopy structure and biomass in a neotropical rainforest. *Remote Sensing of Environment*, **81**, 378–
520 392.

521 Dubayah, R.O., Blair, J.B., Goetz, S., Fatoyinbo, L., Hansen, M., Healey, S., Hofton, M., Hurtt, G., Kellner,
522 J., Luthcke, S., Armston, J., Tang, H., Duncanson, L., Hancock, S., Jantz, P., Marselis, S., Patterson, P.,
523 Qi, W. & Silva, C. The Global Ecosystem Dynamics Investigation: High-resolution laser ranging of
524 the Earth’s forests and topography. *Science of Remote Sensing*.

525 Faith, D.P., Minchin, P.R. & Belbin, L. (1987) Compositional dissimilarity as a robust measure of
526 ecological distance. *Vegetatio*, **69**, 57–68.

527 Fatoyinbo, T.E., Pinto, N., Simard, M., Armston, J., Duncanson, L., Hofton, M., Saatchi, S., Lavalley, M.,
528 Lou, Y., Denbina, M., Dubayah, R., Marselis, S.M., Tang, H., Hancock, S. & Hensley, S. (2017) The
529 2016 NASA AfriSAR campaign: airborne SAR and Lidar measurements of tropical forest structure
530 and biomass in support of future satellite missions. *IEEE Journal of Selected Topics in Applied Earth*
531 *Observations and Remote Sensing*, 4286–4287.

532 Féret, J.B. & Asner, G.P. (2014) Mapping tropical forest canopy diversity using high-fidelity imaging
533 spectroscopy. *Ecological Applications*, **24**, 1289–1296.

534 Foody, G.M. & Cutler, M.E.J. (2006) Mapping the species richness and composition of tropical forests
535 from remotely sensed data with neural networks. *Ecological Modelling*, **195**, 37–42.

536 Gaston, K.J. (2000) Global patterns in biodiversity. *Nature*, **405**, 220–227.

537 Gatti, R.C., Di Paola, A., Bombelli, A., Noce, S. & Valentini, R. (2017) Exploring the relationship between
538 canopy height and terrestrial plant diversity. *Plant Ecology*, **218**, 899–908.

539 Givnish, T.J. (1999) On the causes of gradients in tropical tree diversity. *Journal of Ecology*, **87**, 193–210.

540 Gotelli, N.J. & Colwell, R.K. (2001) Quantifying biodiversity: procedures and pitfalls in the measurement
541 and comparison of species richness. *Ecology Letters*, **4**, 379–391.

542 Hancock, S., Armston, J., Hofton, M., Sun, X., Tang, H., Duncanson, L.I., Kellner, J.R. & Dubayah, R. (2019)
543 The GEDI Simulator: A Large-Footprint Waveform Lidar Simulator for Calibration and Validation of
544 Spaceborne Missions. *Earth and Space Science*, **6**, 294–310.

545 Jucker, T., Asner, G.P., Dalponte, M., Brodrick, P.G., Philipson, C.D., Vaughn, N.R., Arn Teh, Y., Brelsford,
546 C., Burslem, D.F.R.P., Deere, N.J., Ewers, R.M., Kvasnica, J., Lewis, S.L., Malhi, Y., Milne, S., Nilus, R.,
547 Pfeifer, M., Phillips, O.L., Qie, L., Renneboog, N., Reynolds, G., Riutta, T., Struebig, M.J., Svátek, M.,
548 Turner, E.C. & Coomes, D.A. (2018) Estimating aboveground carbon density and its uncertainty in
549 Borneo’s structurally complex tropical forests using airborne laser scanning. *Biogeosciences*, **15**,
550 3811–3830.

- 551 Kearsley, E., De Haulleville, T., Hufkens, K., Kidimbu, A., Toirambe, B., Baert, G., Huygens, D., Kebede, Y.,
552 Defourny, P., Bogaert, J., Beeckman, H., Steppe, K., Boeckx, P. & Verbeeck, H. (2013) Conventional
553 tree height-diameter relationships significantly overestimate aboveground carbon stocks in the
554 Central Congo Basin. *Nature Communications*, **4**.
- 555 Keil, P. & Chase, J.M. (2019) Global patterns and drivers of tree diversity integrated across a continuum
556 of spatial grains. *Nature Ecology and Evolution*, **3**, 390.
- 557 Kier, G., Mutke, J., Dinerstein, E., Ricketts, T.H., Küper, W., Kreft, H. & Barthlott, W. (2005) Global
558 patterns of plant diversity and floristic knowledge. *Journal of Biogeography*, **32**, 1107–1116.
- 559 Labrière, N., Tao, S., Chave, J., Scipal, K., Le Toan, T., Abernethy, K., Alonso, A., Barbier, N., Bissiengou, P.,
560 Casal, T. & others (2018) In Situ Reference Datasets From the TropiSAR and AfriSAR Campaigns in
561 Support of Upcoming Spaceborne Biomass Missions. *IEEE Journal of Selected Topics in Applied*
562 *Earth Observations and Remote Sensing*, 1–11.
- 563 Lewis, S.L., Edwards, D.P. & Galbraith, D. (2015) Increasing human dominance of tropical forests.
564 *Science*, **349**.
- 565 Liang, J., Crowther, T.W., Picard, N., Wiser, S., Zhou, M., Alberti, G., Schulze, E.D., McGuire, A.D.,
566 Bozzato, F., Pretzsch, H., De-Miguel, S., Paquette, A., Hérault, B., Scherer-Lorenzen, M., Barrett,
567 C.B., Glick, H.B., Hengeveld, G.M., Nabuurs, G.J., Pfautsch, S., Viana, H., Vibrans, A.C., Ammer, C.,
568 Schall, P., Verbyla, D., Tchebakova, N., Fischer, M., Watson, J. V., Chen, H.Y.H., Lei, X., Schelhaas,
569 M.J., Lu, H., Gianelle, D., Parfenova, E.I., Salas, C., Lee, E., Lee, B., Kim, H.S., Bruelheide, H., Coomes,
570 D.A., Piotto, D., Sunderland, T., Schmid, B., Gourlet-Fleury, S., Sonké, B., Tavani, R., Zhu, J., Brandl,
571 S., Vayreda, J., Kitahara, F., Searle, E.B., Neldner, V.J., Ngugi, M.R., Baraloto, C., Frizzera, L., Bałazy,
572 R., Oleksyn, J., Zawila-Niedźwiecki, T., Bouriaud, O., Bussotti, F., Finér, L., Jaroszewicz, B., Jucker, T.,
573 Valladares, F., Jagodzinski, A.M., Peri, P.L., Gonmadje, C., Marthy, W., O'Brien, T., Martin, E.H.,
574 Marshall, A.R., Rovero, F., Bitariho, R., Niklaus, P.A., Alvarez-Loayza, P., Chamuya, N., Valencia, R.,
575 Mortier, F., Wortel, V., Engone-Obiang, N.L., Ferreira, L. V., Odeke, D.E., Vasquez, R.M., Lewis, S.L.
576 & Reich, P.B. (2016) Positive biodiversity-productivity relationship predominant in global forests.
577 *Science*.
- 578 Lobo, E. & Dalling, J.W. (2013) Effects of topography, soil type and forest age on the frequency and size
579 distribution of canopy gap disturbances in a tropical forest. *Biogeosciences*, **10**, 6769–6781.
- 580 MacArthur, R.H. & Wilson, E.O. (1967) *The theory of Island Biogeography*, Princeton University Press,
581 Princeton and Oxford.
- 582 Marselis, S.M., Tang, H., Armston, J., Abernethy, K., Alonso, A., Barbier, N., Bissiengou, P., Jeffery, K.,
583 Kenfack, D., Labrière, N. & others (2019) Exploring the relation between remotely sensed vertical
584 canopy structure and tree species diversity in Gabon. *Environmental Research Letters*, **14**.
- 585 Marselis, S.M., Tang, H., Armston, J.D., Calders, K., Labrière, N. & Dubayah, R. (2018) Distinguishing
586 vegetation types with airborne waveform lidar data in a tropical forest-savanna mosaic: A case
587 study in Lopé National Park, Gabon. *Remote Sensing of Environment*, **216**, 626–634.

- 588 Matsunaga, T., Iwasaki, A., Tsuchida, S., Tani, J., Kashimura, O., Nakamura, R., Yamamoto, H.,
589 Tachikawa, T. & Rokugawa, S. (2013) *Current status of Hyperspectral Imager Suite (HISUI).*
590 *International Geoscience and Remote Sensing Symposium (IGARSS)*,.
- 591 Memiaghe, H.R., Lutz, J.A., Korte, L., Alonso, A. & Kenfack, D. (2016) Ecological Importance of Small-
592 Diameter Trees to the Structure, Diversity and Biomass of a Tropical Evergreen Forest at Rabi,
593 Gabon. *PLoS ONE*, **11**.
- 594 Moles, A.T., Warton, D.I., Warman, L., Swenson, N.G., Laffan, S.W., Zanne, A.E., Pitman, A., Hemmings,
595 F.A. & Leishman, M.R. (2009) Global patterns in plant height. *Journal of Ecology*, **97**, 923–932.
- 596 Mutke, J. & Barthlott, W. (2005) Patterns of vascular plant diversity at continental to global scales.
597 *Biologische skrifter*, **55**, 521–531.
- 598 Newnham, G.J., Armston, J.D., Calders, K., Disney, M.I., Lovell, J.L., Schaaf, C.B., Strahler, A.H. & Danson,
599 F.M. (2015) Terrestrial laser scanning for plot-scale forest measurement. *Current Forestry Reports*,
600 **1**, 239–251.
- 601 Palace, M.W., Sullivan, F.B., Ducey, M.J., Treuhaft, R.N., Herrick, C., Shimbo, J.Z. & Mota-E-Silva, J. (2015)
602 Estimating forest structure in a tropical forest using field measurements, a synthetic model and
603 discrete return lidar data. *Remote Sensing of Environment*, **161**, 1–11.
- 604 Pereira, H.M., Ferrier, S., Walters, M., Geller, G.N., Jongman, R.H.G., Scholes, R.J., Bruford, M.W.,
605 Brummitt, N., Butchart, S.H.M., Cardoso, A.C., Coops, N.C., Dulloo, E., Faith, D.P., Freyhof, J.,
606 Gregory, R.D., Heip, C., Höft, R., Hurtt, G., Jetz, W., Karp, D.S., McGeoch, M.A., Obura, D., Onoda,
607 Y., Pettorelli, N., Reyers, B., Sayre, R., Scharlemann, J.P.W., Stuart, S.N., Turak, E., Walpole, M. &
608 Wegmann, M. (2013) Essential biodiversity variables. *Science*, **339**, 277–278.
- 609 Pereira, H.M., Leadley, P.W., Proenca, V., Alkemade, R., Scharlemann, J.P.W., Fernandez-Manjarres, J.F.,
610 Araujo, M.B., Balvanera, P., Biggs, R., Cheung, W.W.L., Chini, L., Cooper, H.D., Gilman, E.L.,
611 Guenette, S., Hurtt, G.C., Huntington, H.P., Mace, G.M., Oberdorff, T., Revenga, C., Rodrigues, P.,
612 Scholes, R.J., Sumaila, U.R. & Walpole, M. (2010) Scenarios for Global Biodiversity in the 21st
613 Century. *Science*, **330**, 1496–1501.
- 614 Pimm, S.L., Jenkins, C.N., Abell, R., Brooks, T.M., Gittleman, J.L., Joppa, L.N., Raven, P.H., Roberts, C.M. &
615 Sexton, J.O. (2014) The biodiversity of species and their rates of extinction, distribution, and
616 protection. *Science*, **344**.
- 617 Piñeiro, G., Perelman, S., Guerschman, J.P. & Paruelo, J.M. (2008) How to evaluate models: Observed vs.
618 predicted or predicted vs. observed? *Ecological Modelling*, **216**, 316–322.
- 619 Qi, W., Saarela, S., Armston, J., Stahl, G. & Dubayah, R. (2019) Forest biomass estimation over three
620 distinct forest types using TanDEM-X InSAR data and simulated GEDI lidar data. *Remote Sensing of*
621 *Environment*, **232**.
- 622 Réjou-Méchain, M., Muller-Landau, H.C., Detto, M., Thomas, S.C., Le Toan, T., Saatchi, S.S., Barreto-Silva,
623 J.S., Bourg, N.A., Bunyavejchewin, S., Butt, N., Brockelman, W.Y., Cao, M., Cárdenas, D., Chiang,

624 J.M., Chuyong, G.B., Clay, K., Condit, R., Dattaraja, H.S., Davies, S.J., Duque, A., Esufali, S., Ewango,
625 C., Fernando, R.H.S., Fletcher, C.D., N. Gunatilleke, I.A.U., Hao, Z., Harms, K.E., Hart, T.B., Hérault,
626 B., Howe, R.W., Hubbell, S.P., Johnson, D.J., Kenfack, D., Larson, A.J., Lin, L., Lin, Y., Lutz, J.A.,
627 Makana, J.R., Malhi, Y., Marthens, T.R., Mcewan, R.W., Mcmahon, S.M., Mcshea, W.J., Muscarella,
628 R., Nathalang, A., Noor, N.S.M., Nytch, C.J., Oliveira, A.A., Phillips, R.P., Pongpattananurak, N.,
629 Punchi-Manage, R., Salim, R., Schurman, J., Sukumar, R., Suresh, H.S., Suwanvecho, U., Thomas,
630 D.W., Thompson, J., Uriarte, M., Valencia, R., Vicentini, A., Wolf, A.T., Yap, S., Yuan, Z., Zartman,
631 C.E., Zimmerman, J.K. & Chave, J. (2014) Local spatial structure of forest biomass and its
632 consequences for remote sensing of carbon stocks. *Biogeosciences*, **11**, 6827–6840.

633 Rocchini, D., Boyd, D.S., Féret, J.B., Foody, G.M., He, K.S., Lausch, A., Nagendra, H., Wegmann, M. &
634 Pettorelli, N. (2016) Satellite remote sensing to monitor species diversity: potential and pitfalls.
635 *Remote Sensing in Ecology and Conservation*, **2**, 25–36.

636 Schäfer, E., Heiskanen, J., Heikinheimo, V. & Pellikka, P. (2016) Mapping tree species diversity of a
637 tropical montane forest by unsupervised clustering of airborne imaging spectroscopy data.
638 *Ecological Indicators*, **64**, 49–58.

639 Skidmore, A.K., Pettorelli, N., Coops, N.C., Geller, G.N., Hansen, M., Lucas, R., Mucher, C.A., O’Connor, B.,
640 Paganini, M., Pereira, H.M., Schaepman, M.E., Turner, W., Wang, T.J. & Wegmann, M. (2015) Agree
641 on biodiversity metrics to track from space. *Nature*, **523**, 403–405.

642 Slik, J.W.F., Arroyo-Rodríguez, V., Aiba, S.-I., Alvarez-Loayza, P., Alves, L.F., Ashton, P., Balvanera, P.,
643 Bastian, M.L., Bellingham, P.J., van den Berg, E., Bernacci, L., da Conceição Bispo, P., Blanc, L.,
644 Böhning-Gaese, K., Boeckx, P., Bongers, F., Boyle, B., Bradford, M., Brearley, F.Q., Breuer-
645 Ndoundou Hockemba, M., Bunyavejchewin, S., Calderado Leal Matos, D., Castillo-Santiago, M.,
646 Catharino, E.L.M., Chai, S.-L., Chen, Y., Colwell, R.K., Chazdon, R.L., Clark, C., Clark, D.B., Clark, D.A.,
647 Culmsee, H., Damas, K., Dattaraja, H.S., Dauby, G., Davidar, P., DeWalt, S.J., Doucet, J.-L., Duque, A.,
648 Durigan, G., Eichhorn, K.A.O., Eisenlohr, P. V., Eler, E., Ewango, C., Farwig, N., Feeley, K.J., Ferreira,
649 L., Field, R., de Oliveira Filho, A.T., Fletcher, C., Forshed, O., Franco, G., Fredriksson, G., Gillespie, T.,
650 Gillet, J.-F., Amarnath, G., Griffith, D.M., Grogan, J., Gunatilleke, N., Harris, D., Harrison, R., Hector,
651 A., Homeier, J., Imai, N., Itoh, A., Jansen, P.A., Joly, C.A., de Jong, B.H.J., Kartawinata, K., Kearsley,
652 E., Kelly, D.L., Kenfack, D., Kessler, M., Kitayama, K., Kooyman, R., Larney, E., Laumonier, Y.,
653 Laurance, S., Laurance, W.F., Lawes, M.J., Amaral, I.L. do, Letcher, S.G., Lindsell, J., Lu, X., Mansor,
654 A., Marjokorpi, A., Martin, E.H., Meilby, H., Melo, F.P.L., Metcalfe, D.J., Medjibe, V.P., Metzger, J.P.,
655 Millet, J., Mohandass, D., Montero, J.C., de Morisson Valeriano, M., Mugerwa, B., Nagamasu, H.,
656 Nilus, R., Ochoa-Gaona, S., Onrizal, Page, N., Parolin, P., Parren, M., Parthasarathy, N., Paudel, E.,
657 Permana, A., Piedade, M.T.F., Pitman, N.C.A., Poorter, L., Poulsen, A.D., Poulsen, J., Powers, J.,
658 Prasad, R.C., Puyravaud, J.-P., Razafimahaimodison, J.-C., Reitsma, J., dos Santos, J.R., Roberto
659 Spironello, W., Romero-Saltos, H., Rovero, F., Rozak, A.H., Ruokolainen, K., Rutishauser, E., Saiter,
660 F., Saner, P., Santos, B.A., Santos, F., Sarker, S.K., Satdichanh, M., Schmitt, C.B., Schöngart, J.,
661 Schulze, M., Suganuma, M.S., Sheil, D., da Silva Pinheiro, E., Sist, P., Stevart, T., Sukumar, R., Sun, I.-
662 F., Sunderland, T., Suresh, H.S., Suzuki, E., Tabarelli, M., Tang, J., Targhetta, N., Theilade, I., Thomas,
663 D.W., Tchouto, P., Hurtado, J., Valencia, R., van Valkenburg, J.L.C.H., Van Do, T., Vasquez, R.,

664 Verbeeck, H., Adekunle, V., Vieira, S.A., Webb, C.O., Whitfeld, T., Wich, S.A., Williams, J., Wittmann,
665 F., Wöll, H., Yang, X., Adou Yao, C.Y., Yap, S.L., Yoneda, T., Zahawi, R.A., Zakaria, R., Zang, R., de
666 Assis, R.L., Garcia Luize, B. & Venticinque, E.M. (2015) An estimate of the number of tropical tree
667 species. *Proceedings of the National Academy of Sciences*, **112**, 7472–7477.

668 Slik, J.W.F., Franklin, J., Arroyo-Rodríguez, V., Field, R., Aguilar, S., Aguirre, N., Ahumada, J., Aiba, S.I.,
669 Alves, L.F., Anitha, K., Avella, A., Mora, F., Aymard, G.A.C., Báez, S., Balvanera, P., Bastian, M.L.,
670 Bastin, J.F., Bellingham, P.J., Van Den Berg, E., Da Conceição Bispo, P., Boeckx, P., Boehning-Gaese,
671 K., Bongers, F., Boyle, B., Brambach, F., Brearley, F.Q., Brown, S., Chai, S.L., Chazdon, R.L., Chen, S.,
672 Chhang, P., Chuyong, G., Ewango, C., Coronado, I.M., Cristóbal-Azkarate, J., Culmsee, H., Damas, K.,
673 Dattaraja, H.S., Davidar, P., DeWalt, S.J., DiN, H., Drake, D.R., Duque, A., Durigan, G., Eichhorn, K.,
674 Eler, E.S., Enoki, T., Ensslin, A., Fandohan, A.B., Farwig, N., Feeley, K.J., Fischer, M., Forshed, O.,
675 Garcia, Q.S., Garkoti, S.C., Gillespie, T.W., Gillet, J.F., Gonmadje, C., Granzow-De La Cerda, I.,
676 Griffith, D.M., Grogan, J., Hakeem, K.R., Harris, D.J., Harrison, R.D., Hector, A., Hemp, A., Homeier,
677 J., Hussain, M.S., Ibarra-Manríquez, G., Hanum, I.F., Imai, N., Jansen, P.A., Joly, C.A., Joseph, S.,
678 Kartawinata, K., Kearsley, E., Kelly, D.L., Kessler, M., Killeen, T.J., Kooyman, R.M., Laumonier, Y.,
679 Laurance, S.G., Laurance, W.F., Lawes, M.J., Letcher, S.G., Lindsell, J., Lovett, J., Lozada, J., Lu, X.,
680 Lykke, A.M., Bin Mahmud, K., Mahayani, N.P.Di., Mansor, A., Marshall, A.R., Martin, E.H., Matos,
681 D.C.L., Meave, J.A., Melo, F.P.L., Mendoza, Z.H.A., Metali, F., Medjibe, V.P., Metzger, J.P., Metzker,
682 T., Mohandass, D., Munguía-Rosas, M.A., Muñoz, R., Nurtjahya, E., De Oliveira, E.L., Onrizal,
683 Parolin, P., Parren, M., Parthasarathy, N., Paudel, E., Perez, R., Pérez-García, E.A., Pommer, U.,
684 Poorter, L., Qi, L., Piedade, M.T.F., Pinto, J.R.R., Poulsen, A.D., Poulsen, J.R., Powers, J.S., Prasad,
685 R.C., Puyravaud, J.P., Rangel, O., Reitsma, J., Rocha, Di.S.B., Rolim, S., Rovero, F., Rozak, A.,
686 Ruokolainen, K., Rutishauser, E., Rutten, G., Mohd Said, M.N., Saiter, F.Z., Saner, P., Santos, B., Dos
687 Santos, J.R., Sarker, S.K., Schmitt, C.B., Schoengart, J., Schulze, M., Sheil, D., Sist, P., Souza, A.F.,
688 Spironello, W.R., Sposito, T., Steinmetz, R., Stevart, T., Suganuma, M.S., Sukri, R., Sultana, A.,
689 Sukumar, R., Sunderland, T., Supriyadi, Suresh, H.S., Suzuki, E., Tabarelli, M., Tang, J., Tanner, E.V.J.,
690 Targhetta, N., Theilade, I., Thomas, D., Timberlake, J., De Morisson Valeriano, M., Van Valkenburg,
691 J., Van Do, T., Van Sam, H., Vandermeer, J.H., Verbeeck, H., Vetaas, O.R., Adekunle, V., Vieira, S.A.,
692 Webb, C.O., Webb, E.L., Whitfeld, T., Wich, S., Williams, J., Wisser, S., Wittmann, F., Yang, X., Yao,
693 C.Y.A., Yap, S.L., Zahawi, R.A., Zakaria, R. & Zang, R. (2018) Phylogenetic classification of the world's
694 tropical forests. *Proceedings of the National Academy of Sciences of the United States of America*,
695 **115**, 1837–1842.

696 Ter Steege, H., Pitman, N.C.A., Killeen, T.J., Laurance, W.F., Peres, C.A., Guevara, J.E., Salomão, R.P.,
697 Castilho, C. V., Amaral, I.L., de Almeida Matos, F.D. & others (2015) Estimating the global
698 conservation status of more than 15,000 Amazonian tree species. *Science advances*, **1**, e1500936.

699 Sullivan, M.J.P., Talbot, J., Lewis, S.L., Phillips, O.L., Qie, L., Begne, S.K., Chave, J., Cuni-Sanchez, A.,
700 Hubau, W., Lopez-Gonzalez, G., Miles, L., Monteagudo-Mendoza, A., Sonké, B., Sunderland, T., Ter
701 Steege, H., White, L.J.T., Affum-Baffoe, K., Aiba, S.I., De Almeida, E.C., De Oliveira, E.A., Alvarez-
702 Loayza, P., Dávila, E.Á., Andrade, A., Aragão, L.E.O.C., Ashton, P., Aymard, G.A., Baker, T.R., Balinga,
703 M., Banin, L.F., Baraloto, C., Bastin, J.F., Berry, N., Bogaert, J., Bonal, D., Bongers, F., Brienens, R.,

704 Camargo, J.L.C., Cerón, C., Moscoso, V.C., Chezeaux, E., Clark, C.J., Pacheco, Á.C., Comiskey, J.A.,
705 Valverde, F.C., Coronado, E.N.H., Dargie, G., Davies, S.J., De Canniere, C., Djuikouo, M.N., Doucet,
706 J.L., Erwin, T.L., Espejo, J.S., Ewango, C.E.N., Fauset, S., Feldpausch, T.R., Herrera, R., Gilpin, M.,
707 Gloor, E., Hall, J.S., Harris, D.J., Hart, T.B., Kartawinata, K., Kho, L.K., Kitayama, K., Laurance, S.G.W.,
708 Laurance, W.F., Leal, M.E., Lovejoy, T., Lovett, J.C., Lukasu, F.M., Makana, J.R., Malhi, Y.,
709 Maracahipes, L., Marimon, B.S., Junior, B.H.M., Marshall, A.R., Morandi, P.S., Mukendi, J.T.,
710 Mukinzi, J., Nilus, R., Vargas, P.N., Camacho, N.C.P., Pardo, G., Peña-Claros, M., Pétronelli, P.,
711 Pickavance, G.C., Poulsen, A.D., Poulsen, J.R., Primack, R.B., Priyadi, H., Quesada, C.A., Reitsma, J.,
712 Réjou-Méchain, M., Restrepo, Z., Rutishauser, E., Salim, K.A., Salomão, R.P., Samsedin, I., Sheil, D.,
713 Sierra, R., Silveira, M., Slik, J.W.F., Steel, L., Taedoumg, H., Tan, S., Terborgh, J.W., Thomas, S.C.,
714 Toledo, M., Umunay, P.M., Gamarra, L.V., Vieira, I.C.G., Vos, V.A., Wang, O., Willcock, S. &
715 Zemagho, L. (2017) Diversity and carbon storage across the tropical forest biome. *Scientific*
716 *Reports*, **7**, 39102.

717 Tang, H., Dubayah, R., Swatantran, A., Hofton, M., Sheldon, S., Clark, D.B. & Blair, B. (2012) Retrieval of
718 vertical LAI profiles over tropical rain forests using waveform lidar at La Selva, Costa Rica. *Remote*
719 *Sensing of Environment*, **124**, 242–250.

720 Le Toan, T., Quegan, S., Davidson, M.W.J., Balzter, H., Paillou, P., Papathanassiou, K., Plummer, S., Rocca,
721 F., Saatchi, S., Shugart, H. & Ulander, L. (2011) The BIOMASS mission: Mapping global forest
722 biomass to better understand the terrestrial carbon cycle. *Remote Sensing of Environment*.

723 Watson, J.E.M., Darling, E.S., Venter, O., Maron, M., Walston, J., Possingham, H.P., Dudley, N., Hockings,
724 M., Barnes, M. & Brooks, T.M. (2016) Bolder science needed now for protected areas. *Conservation*
725 *Biology*, **30**, 243–248.

726 Watson, J.E.M., Evans, T., Venter, O., Williams, B., Tulloch, A., Stewart, C., Thompson, I., Ray, J.C.,
727 Murray, K., Salazar, A., McAlpine, C., Potapov, P., Walston, J., Robinson, J.G., Painter, M., Wilkie, D.,
728 Filardi, C., Laurance, W.F., Houghton, R.A., Maxwell, S., Grantham, H., Samper, C., Wang, S.,
729 Laestadius, L., Runting, R.K., Silva-Chávez, G.A., Ervin, J. & Lindenmayer, D. (2018) The exceptional
730 value of intact forest ecosystems. *Nature Ecology and Evolution*, **2**, 599.

731 Wolf, J.A., Fricker, G.A., Meyer, V., Hubbell, S.P., Gillespie, T.W. & Saatchi, S.S. (2012) Plant species
732 richness is associated with canopy height and topography in a neotropical forest. *Remote Sensing*,
733 **4**, 4010–4021.

734

735 **Data Availability Statement**

736 Some of the field and lidar data used in this study can be downloaded directly from the internet. We
737 have grouped the data in three groups here: (i) LVIS lidar data, (ii) ALS lidar data and (iii) field data. All
738 datasets not mentioned in this statement were previously collected but have not been made publicly
739 available and were accessed through personal collaboration with the data providers.

740 **(i) LVIS lidar data**

741 The LVIS data for the *rab*, *lop*, *mon* and *mab* study sites can be downloaded from the NASA data archive
742 at the following DOI: <https://doi.org/10.3334/ORNLDAAC/1591>.

743 The LVIS data for the *cha* and *lsv* study sites is available on the following website:

744 <https://lvis.gsfc.nasa.gov/Data/Maps/CR2005Map.html>.

745 **(ii) ALS lidar data**

746 The ALS data over *rob* is available through the auscover data portal

747 ftp://gld.auscover.org.au/airborne_validation/lidar/robsons_creek/.

748 The ALS data over *s11* and *s12* can be downloaded from the sustainable landscapes data portal

749 <http://www.paisagenslidar.cnptia.embrapa.br/webgis/>.

750 **(iii) Field data**

751 Field data from *rob* has been published through the Terrestrial Ecosystem Research Network (TERN)

752 data portal linked from <https://supersites.tern.org.au/supersites/fnqr-robson>.

753 The *dan* and *rab* field data are all available through the Forestgeo website at

754 <https://forestgeo.si.edu/sites/asia/danum-valley>, <https://forestgeo.si.edu/sites/africa/rabi> and

755 <https://forestgeo.si.edu/sites/neotropics/barro-colorado-island>.

756 The *sep*, *lop* and *tam* field data are all available through forestplots.net and can be found under the
757 project names 'sepilok', 'lope' and 'tambopata' at <https://www.forestplots.net/en/>.

758 The *mon* field data is archived through the NASA data archiving center and available at DOI:
759 <https://doi.org/10.3334/ORNLDACC/1580>.

760 The *s11* and *s12* were available through the data portals of the sustainable landscapes projects and can
761 be found under the field data from the São Félix do Xingu region collected in 2011 and 2012 in the
762 following data portal: <http://www.paisagenslidar.cnptia.embrapa.br/webgis/>.